Interpretable POLSAR Image Classification Based on Adaptive-Dimension Feature Space Decision Tree

QIANG YIN[1], **(Member, IEEE), JIANDA CHENG**[1], **FAN ZHANG**[1], **(Senior Member, IEEE),**
YONGSHENG ZHOU[1], **(Member, IEEE), LUYI SHAO**[2], **AND**
WEN HONG[3], **(Senior Member, IEEE)**

[1]College of Information Science and Technology, Beijing University of Chemical Technology, Beijing 100029, China
[2]College of Information Science and Engineering, Ocean University of China, Qingdao 266100, China
[3]Institute of Electronics, Chinese Academy of Sciences, Beijing 100190, China

Corresponding author: Jianda Cheng (chengjd4152@163.com)

ABSTRACT Decision tree method has been applied to POLSAR image classification, due to its capability to interpret the scattering characteristics as well as good classification accuracy. Compared with popular machine learning classifiers, decision tree approach can explain the scattering process of certain type of targets by use of the polarimetric features at the tree nodes. Except the interpretability, decision tree approach could be transplanted to other data set without training process for the same terrain types, since the polarimetric features are inherently connected to the physical scattering properties. Currently, decision tree based classifiers, typically employ one single polarimetric feature at the nodes of the tree. The idea to increase the number of the polarization features at the decision tree node is expected to improve the classification result, which combine two or more polarimetric features to form a two or high dimension feature space. In this way, the classes which cannot be discriminated with one feature could possibly be separated with the space constructed by several features. However, it also inevitably leads to an increase in the computational burden. In fact, not all nodes require very high-dimensional feature space to achieve high classification precision. Therefore, in this article we proposed that the dimension of the feature space used in the decision tree nodes is adaptively changed from one to three, due to the separability of the classes under this node. The developed classification method is examined by the classical AIRSAR data in Flevoland area of the Netherlands, as well as GaoFen-3 data in Hulunbuir of China. The experiments show that the classification performance is superior to the fixed dimension feature decision tree methods, with less and reasonable computation time. Besides, the transferability of polarimetric features obtained by decision tree is preliminarily demonstrated in the application to another AIRSAR data.

INDEX TERMS Polarimetric SAR, feature space, decision tree, terrain classification.

I. INTRODUCTION

Polarimetric Synthetic Aperture Radar (POLSAR) is a multi-parameter, multi-channel microwave imaging radar system, which is widely used in vegetation distribution [1], ocean research [2], [3], disaster assessment [4], [5] and so on. The backscatter information of POLSAR contains the complex scattering mechanism of the observed target [6]. For example, the geometry, dielectric constant and roughness of scatterers

are closely related to the scattering mechanism. Polarization can distinguish basic scattering mechanisms, such as volume scattering, double-bounce scattering, surface scattering and so on. However, the scatterers in nature often exhibit complicated scattering characteristics, so describing the scattering mechanism of target is a difficult and important research topic in the application of POLSAR images.

Polarimetric features are useful information extracted from complex scattering mechanisms, which include the geometric structure, distribution direction, dielectric property, and so on of targets. How to interpret and utilize polarimetric

features has become one of the central tasks of POLSAR image processing [7]. Combining polarimetric features with different classification methods to achieve more effective PolSAR image classification is an important research field. According to whether there exists data label and manual intervention, the classification methods can be mainly divided into two types, supervised and unsupervised methods. The unsupervised classification methods classify data according to their statistical characteristics without prior knowledge, such as complex Wishart [8]–[10], k-means clustering [11], [12], fuzzy c-means clustering [13], Expectation Maximization [14] and so on. The unsupervised classification methods cannot obtain satisfactory classification accuracy, when the difference in scattering characteristics of targets is small. There are a lot of supervised classification methods have been proposed, such as Support Vector Machine (SVM) [15], Random Forest (RF) [16], [17], deep learning [18], [19], Nearest-Regularized Subspace(NRS) [20] and so on [21]. Although the differences of polarimetric features are used to classify targets in these supervised classification methods, which are data-driven, the scattering characteristics of targets are not mapped to the certain features.

Compared to those popular machine learning and deep learning methods, the classical decision tree approach has its own advantages over several aspects. By reviewing the related work in the literature, the advantages are briefly summarized as follows:

1) Interpretability: The polarimetric radar data could capture the geometrical and bio-physical information about targets, which is the key capability for realizing unsupervised classification. Geometrical and bio-physical properties of targets decide their radar scattering process. In the decision tree method, the polarimetric features used in the tree nodes for discriminating certain categories are clear, so it is possible explain the scattering characteristics of these categories.

2) Transferability: Generally, the observation capability of the certain POLSAR sensor keeps stable, hence the polarimetric features for classification can be probably applied to the data in different area acquired by the same sensor, without training process. Furthermore, for different sensor data, it is also possible to be utilized in a proper way, because the similar targets also show close scattering properties and polarimetric features as well.

3) Adjustability: The hierarchical structure of decision tree presents the role of the used polarimetric features, as well as their relations with terrain types, thus we could increase the classification accuracy of our concerned type through adjusting the tree structure such as branch order or employed features, according to the needs in reality.

At present, almost all decision tree based classifiers employ only one single polarimetric feature at the nodes of the decision tree. Zhang *et al.* used one-dimensional feature decision tree to classify crops and explained the scattering mechanism of crops through the classification results [22]. Zhang and Yan inputted 72 polarimetric features to establish a one-dimensional feature decision tree, and pointed out that with the increase of polarization characteristics, the useful information for classification may also be increase, and the classification results of terrain objects tend to be accurate [23]. In the [24], Jain and Singh proposed a decision-tree-based approach for land cover classification of Radarsat-2 data, multiple inequalities containing polarimetric parameters are used, but no feature space is formed. Thakur *et al.* developed a decision tree based on separability index to classify ALOS-PALSAR data [25]. And G. S. Phartiyal *et al.* attempt to analyze the polarimetric signature to decide the individual class boundary values which will help in building a decision tree based classification technique [26]. Those above methods focus on the feature selection or optimization before decision tree algorithm, not on the improvement on the tree nodes.

In the field of decision tree application, the focus of research is mostly on extending feature set, but the nodes of decision tree still adopt one polarimetric feature. Traditional one-dimensional feature decision tree has poor classification ability among targets with similar scattering characteristics. Due to the complexity of the physical properties of the actual targets, they often show more than one kind of mixed scattering characteristics. Therefore, the scattering characteristics of an actual target cannot be explained completely by one polarimetric feature. One dimensional polarimetric feature could discriminate the basic type of scattering mechanism well, such as surface scattering, double-bounce scattering, and volume scattering. However, it could not separate the vegetation very well because almost all the vegetation contains not only volume scattering by branches and leaves, but also some double-bounce scattering mechanisms from the dihedral constructed by soil surface and trunks. Shao and Hong [27] increased the dimension of the decision tree nodes to two and verifies that it can improve the accuracy of classification. As the number of polarimetric features increases, the separability of classes increase as well, so as the accuracy of classification [28], [29]. In this article, the maximum dimension of decision tree nodes reaches to three, and a classification method of adaptive-dimension feature decision tree is proposed. The dimension of the nodes starts from one, and expands to two or three, depending on the purity of the linearly separable clusters. In the continuously updated training sample set, the Fisher Linear Discriminant analysis [30], [31] was used to project the multidimensional space into one dimension. Then Jeffries-Matusita (J-M) distance [32], [33] is adopted to calculate the thresholds which used to divide the boundary. The determinant of confusion matrix [34] is calculated as purity and the linearly separable clusters are selected with the highest purity. The end of the decision tree branch is decided when there is only one category label in both groups. The proposed classification method is examined by the widely tested AIRSAR data in Flevoland area of the Netherlands, as well as GaoFen-3 data in Hulunbuir of China.

The main contribution of this article is to develop a new decision tree method for POLSAR data classification, in which the dimension of polarimetric feature space is adaptively decided at the tree nodes. Traditional fixed dimensional decision tree approaches are compared with the proposed one, including one to three dimension cases. Besides, classical SVM method is also experimented for comparison. Among them, the method developed in this study shows the best compromise between classification accuracy and computation efficiency. By the use of adaptive dimensional feature space, actually the better features for discriminating certain class groups are founded. It achieves the grained interpretation of similar scattering mechanisms of terrain types, and is preliminarily demonstrated by transplanting the features obtained at the tree nodes directly to another data sets of the same sensor for classification without training process.

In the following sections, the theory and classification methods for this article are described in Section II, the experimental data sets and results analysis are given in Section III, the discussion is given in Section IV, and conclusion is given in Section V.

II. METHODS
A. POLARIMETRIC FEATURES
In this article, eight polarimetric features [27], [35] are selected for the decision tree, as shown in Table 1. The 8 features can be divided into two categories, one is from the second-order backscattering matrix, including $\langle|S_{HH}|^2\rangle$(the backscattering power of HH), $\langle|S_{VV}|^2\rangle$(the backscattering power of VV), $\langle S_{HH}S_{VV}^*\rangle$(the co-polarization cross product), CPR(the ratio of co-polarization component to cross-polarization component) and $Span$(the total backscattering power). And the other is from the polarization decomposition components, including α(the scattering angle), $H(1-A)$(the combination of entropy and anisotropy) and P_V(the volume scattering component from Freeman-Durden decomposition).

TABLE 1. Polarimetric features for decision trees.

f_1	f_2	f_3	f_4	f_5	f_6	f_7	f_8
α	$\langle|S_{HH}|^2\rangle$	$\langle S_{HH}S_{VV}^*\rangle$	$\langle|S_{VV}|^2\rangle$	CPR	$H(1-A)$	P_V	$Span$

In full polarization observation, assuming that the mode of transmission and reception is linear horizontal and vertical polarization, the backscattering matrix $[S]$ is expressed as

$$[S] = \begin{bmatrix} S_{HH} & S_{HV} \\ S_{VH} & S_{VV} \end{bmatrix}, \tag{1}$$

where S_{HH} and S_{VV} contain the backscattering power of the co-polarization channel, S_{HV} and S_{VH} contain the backscattering power of cross-polarized channel. If the transmitted and received signals are transmitted in the medium that satisfies the reciprocity, the backscattering matrix also satisfies the reciprocity theorem, i.e., $S_{HV} = S_{VH}$.

According to the backscattering matrix, and assuming reciprocity, the following three circular polarization components can be derived

$$\begin{cases} S_{RR} = \dfrac{S_{HH} - S_{VV} + iS_{HV}}{2} \\ S_{LL} = \dfrac{S_{VV} - S_{HH} + iS_{HV}}{2} \\ S_{RL} = \dfrac{i(S_{HH} + S_{VV})}{2}, \end{cases} \tag{2}$$

where S_{RR} and S_{LL} represent right-right circular polarization component and left-left circular polarization component respectively, S_{RL} represents right-left circular polarization component.

Circular Polarization Ratio (CPR) can be used to classify three scattering mechanisms, i.e. surface, volume and double-bounce scatterings, respectively [36]. It is defined as

$$CPR = \frac{\langle|S_{RR}|^2\rangle}{\langle|S_{RL}|^2\rangle} = \frac{\langle|S_{HH} - S_{VV}|^2\rangle + 4\langle|S_{HV}|^2\rangle}{\langle|S_{HH} + S_{VV}|^2\rangle}. \tag{3}$$

The polarimetric covariance matrix is derived from the scattering matrix, and assuming reciprocity, it is defined as

$$C_3 = \begin{bmatrix} \langle|S_{HH}|^2\rangle & \sqrt{2}\langle S_{HH}S_{HV}^*\rangle & \langle S_{HH}S_{VV}^*\rangle \\ \sqrt{2}\langle S_{HV}S_{HH}^*\rangle & 2\langle|S_{HV}|^2\rangle & \sqrt{2}\langle S_{HV}S_{VV}^*\rangle \\ \langle S_{VV}S_{HH}^*\rangle & \sqrt{2}\langle S_{VV}S_{HV}^*\rangle & \langle|S_{VV}|^2\rangle \end{bmatrix}, \tag{4}$$

where * represents the complex conjugation, $\langle\cdot\rangle$ represents the ensemble average of time or space, and S_{XY} represents the complex scattering amplitude when the transmitted and received signals have a polarization X and Y, respectively. $\langle|S_{HH}|^2\rangle$ and $\langle|S_{VV}|^2\rangle$ can effectively improve classification accuracy [37]. While $\langle S_{HH}S_{VV}^*\rangle$ could distinguish three types of scattering: single bounce, volume and double bounce scattering [38].

Total scattering power is an important representation of spatial information can be used for image edge extraction, texture analysis etc., which is the sum of the diagonal elements of the covariance matrix.

Cloude and Pottier proposed a eigenvalue based decomposition theory using second-order statistics to extract the average parameters of samples [39]. Three averaged parameters can be derived from the covariance matrix $[C_3]$: mean scattering angle (α), entropy (H), and anisotropy (A), which are defined as

$$\overline{\alpha} = \sum_{k=1}^{3} p_k \alpha_k, \tag{5}$$

$$H = -\sum_{k=1}^{3} p_k \log_3(p_k), \tag{6}$$

$$A = \frac{\lambda_2 - \lambda_3}{\lambda_2 + \lambda_3}, \tag{7}$$

where $p_k = \lambda_k / \sum_{k=1}^{3} \lambda_k$, $(k = 1, 2, 3)$. And the eigenvalues are arranged in order from large to small ($\lambda_1 > \lambda_2 > \lambda_3 > 0$). The mean scattering angle α, ranging from 0° to 90°, describes the continuous variation of scattering mechanism, varying from surface scattering($\alpha \approx 0°$) to dipole scattering($\alpha \approx 45°$) and then to double bounce

scattering($\alpha \approx 90°$). The entropy H, ranging from 0 to 1, represents the randomness of the scatterer from isotropic scattering ($H = 0$) to totally random scattering ($H = 1$). The anisotropy A is very useful for discriminating scattering mechanisms, especially for those with different eigenvalue distributions but similar entropy values. The combination of entropy and anisotropy $H(1 - A)$ represents the random scattering process, which satisfies the high value of H, and the low value of A, which means $\lambda_2 \approx \lambda_3 \approx \lambda_1$.

Freeman-Durden decomposition is an incoherent matrix decomposition method based on three physical scattering models, for surface, dihedral and volume respectively. Assuming that these components of are not correlated, the polarimetric covariance matrix $[C_3]$ can be expressed as

$$
C_3 = \begin{bmatrix} f_S|\beta|^2 + f_D|\alpha|^2 + \frac{3f_V}{8} & 0 & f_S\beta + f_D\alpha + \frac{f_V}{8} \\ 0 & \frac{2f_V}{8} & 0 \\ f_S\beta^* + f_D\alpha^* + \frac{f_V}{8} & 0 & f_S + f_D + \frac{3f_V}{8} \end{bmatrix}, \quad (8)
$$

where f_V, f_S, and f_D is the contribution of volume, surface and double-bounce scattering component. The 5 parameters α, β, f_S and f_D are estimated from the actual radar data. The results of F-D target decomposition are P_S, P_D, and P_V, which represent the power of three scattering mechanism components, respectively.

$$
\begin{aligned}
Span &= \left\langle |S_{HH}|^2 \right\rangle + 2\left\langle |S_{HV}|^2 \right\rangle + \left\langle |S_{VV}|^2 \right\rangle \\
&= P_S + P_D + P_V,
\end{aligned} \quad (9)
$$

where $P_S = f_S\left(1 + |\beta|^2\right)$, $P_D = f_D\left(1 + |\alpha|^2\right)$, $P_V = f_V$.

B. FISHER LINEAR DISCRIMINANT ANALYSIS

When the decision tree nodes employ the feature space instead of the single feature, the feature space needs to be projected to certain direction so as to judge the linear separability of classes. In this article, Fisher Linear Discriminant Analysis (FLD) [30], [31] is adopted to obtain the projection direction with the largest degree of dispersion between classes, and projects the feature space into one dimension. The formula is as follows

$$
y = \omega^T x, \quad (10)
$$

where ω^T is the projection direction.

However, projecting multidimensional space into one dimension will result in loss of data. Originally well-classified classes in the multidimensional space will be severely overlapped after being projected to one dimension. Therefore, Fisher proposed a standard function (Fisher's ratio). The formula is as follows

$$
J(\omega) = \frac{(m_2 - m_1)^2}{S_1^2 + S_2^2}, \quad (11)
$$

where m_1 and m_2 represent the intra-class mean of the projected samples, S_1 and S_2 represent the standard deviations of the intra-class scatters of the projected samples.

C. J-M DISTANCE

In this article, J-M distance [32], [33] is used to calculate the degree of separation between the samples. The range of distance is [0, 2]. "0" means that two sample categories are completely confused while "2" represents two sample categories are completely separated. The J-M distance formula is as follows

$$
J = 2\left(1 - e^{-B}\right), \quad (12)
$$

where B is the Bhattacharya distance

$$
B = \frac{1}{8}(m_1 - m_2)^2 \frac{2}{\sigma_1^2 + \sigma_2^2} + \frac{1}{2}\ln\left[\frac{\sigma_1^2 + \sigma_2^2}{2\sigma_1\sigma_2}\right], \quad (13)
$$

where m_1 and m_2 represent the mean value of two categories, σ_1 and σ_2 represent the standard deviation of them.

When the J-M distance on one feature satisfies a linearly separable condition between two categories, the thresholds of the two categories in this feature can be calculated, according to the Gaussian probability distribution density function

$$
P(x) = P(x|\omega_1) P(\omega_1) + P(x|\omega_2) P(\omega_2), \quad (14)
$$

where ω_1 and ω_2 represent two classes, $P(\omega_1)$ and $P(\omega_2)$ represent the prior probability, and $P(x|\omega_1)$ and $P(x|\omega_2)$ represent the posterior probability. When x_0 is present, and $P(x_0|\omega_1) = P(x_0|\omega_2)$ is established, the two classes have the best separation effect. Therefore, the value can be used as the threshold. The formula for calculating the threshold T is as follows

$$
T = \frac{m_2\sigma_1^2 - m_1\sigma_2^2 \pm \sigma_1\sigma_2\sqrt{(m_1 - m_2)^2 + 2A(\sigma_1^2 - \sigma_2^2)}}{(\sigma_1^2 - \sigma_2^2)}, \quad (15)
$$

where $A = \log_{10}(\frac{\sigma_1}{\sigma_2} \times \frac{m_2}{m_1})$.

D. PROPOSED METHOD

The traditional one-dimensional decision tree cannot satisfy the classification requirement very well, especially has poor classification ability among targets with similar scattering characteristics. Due to the complexity of the physical characteristics of the actual target, it often shows more than one kind of scattering properties. Therefore, selecting several polarimetric features to form feature space at some nodes is not only expected to improve classification accuracy, but also to explain the scattering mechanism of targets more comprehensively. However, when more than three polarimetric features are selected at tree nodes, the computational complexity will increase to an unacceptable level. In this article, an improved decision tree classification method is proposed, and the core part is to construct the adaptive-dimension feature space, which could contain one, two and three dimension. FLD and J-M distances are used as the linear separability measurement and the boundary partition algorithm, and "purity" is used as the branching criterion of the decision tree. Here we adopt the

determinant of the confusion matrix as purity. The confusion matrix $[C]$ is defined as follows:

$$[C] = \begin{bmatrix} c_{11} & c_{12} \\ c_{21} & c_{22} \end{bmatrix}, \tag{16}$$

where c_{11} and c_{22} represent the number of correctly classified samples, c_{12} and c_{21} represent the number of wrong classified ones. Then, the normalized confusion matrix is calculated as purity, i.e. $p = |\widetilde{C}|$. There is no doubt that the more samples are correctly classified, the closer the calculated purity is to "1". The method of calculating the purity, taking into account the number of correctly and incorrectly classified samples, ensures that the combination of terrain types is optimal.

In this article, a classification method of adaptive-dimension decision tree is proposed. At first, we need to construct the decision tree with training samples, then the classification of testing samples with the tree is implemented. The construction of decision tree is as shown in Algorithm. 1, and the diagram of classification with adaptive-dimension decision tree is shown in Fig. 1.

III. EXPERIMENTS

This section consists of three subsections. Subsection III-A introduces the information of experimental data set. Subsection III-B analyses the fine-grained interpretability of the adaptive-dimension feature decision tree. Subsection III-C gives the classification accuracy comparison of different methods.

A. DATA SET

The experimental data set is the widely-used L-band data acquired by NASA/JPL AIRSAR system over the Flevoland test site in mid-August of 1989. The incidence angles are around $20°$ at the near range and $44°$ at the far range. There are 15 different terrain types were marked in the ground truth image, including stem bean, forest, potatoes, alfalfa, wheat, bare soil, beets, rapeseed, peas, grasses, water, barley, buildings, wheat2 and wheat3. The size of the datum is 750×1024 pixels. It is filtered to reduce the speckle noise by using refined Lee filter (7×7 window size). The Pauli image and the ground truth image are shown in Fig. 2. And 5% of the labeled pixels are selected as training pixels. The number of samples is shown in Table 2.

B. FINE-GRAINED INTERPRETABILITY

The decision tree classification method is different from other POLSAR image classification methods, for it retains the polarimetric features used in tree nodes which can be used to describe target scattering mechanism and interpret classification rules. Compared with the classical polarimetric feature decision tree, the proposed method can realize the one-time classification of a single terrain type, that is, a single terrain type only corresponds to one leaf node in the decision tree.

Algorithm 1 Construction of Adaptive-Dimension Decision Tree

Require: Fully polarimetric SAR image
Ensure: Class labels of the entire test image pixels.
1: Preprocessing ← refined Lee filter
2: Feature set ← stack 8 categories of polarimetric features

3: Classification process of the node:
4: $H \leftarrow 1$ (high threshold)
5: $L \leftarrow 0.97$ (low threshold)
6: Construct one-dimensional feature space:
7: **for** each $f \in [1, 8]$ **do**
8: classification result of the node ← J-M distance
9: $p \leftarrow |\widetilde{C}|$ (C: confusion matrix)
10: $purity \leftarrow \max\{p\}$
11: **end for**
12: **if** $purity \geq H$ **then**
13: break
14: **else if** $H \geq purity \geq L$ **then**
15: Construct two-dimensional feature space:
16: **for** each $f_1 \in [1, 8]$ **do**
17: **for** each $f_2 \in [1, 8]$ **do**
18: dimensionality reduction ← FLD
19: classification result of the node ← J-M distance
20: $p \leftarrow |\widetilde{C}|$ (C: confusion matrix)
21: $purity \leftarrow \max\{p\}$
22: **end for**
23: **end for**
24: **else**
25: Construct three-dimensional feature space:
26: **for** each $f_1 \in [1, 8]$ **do**
27: **for** each $f_2 \in [1, 8]$ **do**
28: **for** each $f_2 \in [1, 8]$ **do**
29: dimensionality reduction ← FLD
30: classification result of the node ← J-M distance
31: $p \leftarrow |\widetilde{C}|$ (C: confusion matrix)
32: $purity \leftarrow \max\{p\}$
33: **end for**
34: **end for**
35: **end for**
36: **end if**
37: Select the node with the highest purity for branching
38: **repeat**
39: carry out processing: $3 \sim 37$
40: **until** the node contains only one terrain type

Because of the complexity of the physical characteristics of the actual targets, they often shows more than one kind of mixed scattering phenomena. In this case, if single polarization feature is used at the tree nodes, then the dominant scattering mechanism of the target is identified, and the description of the scattering mechanism for complex areas (such as agricultural regions) is incomplete. Therefore, in this
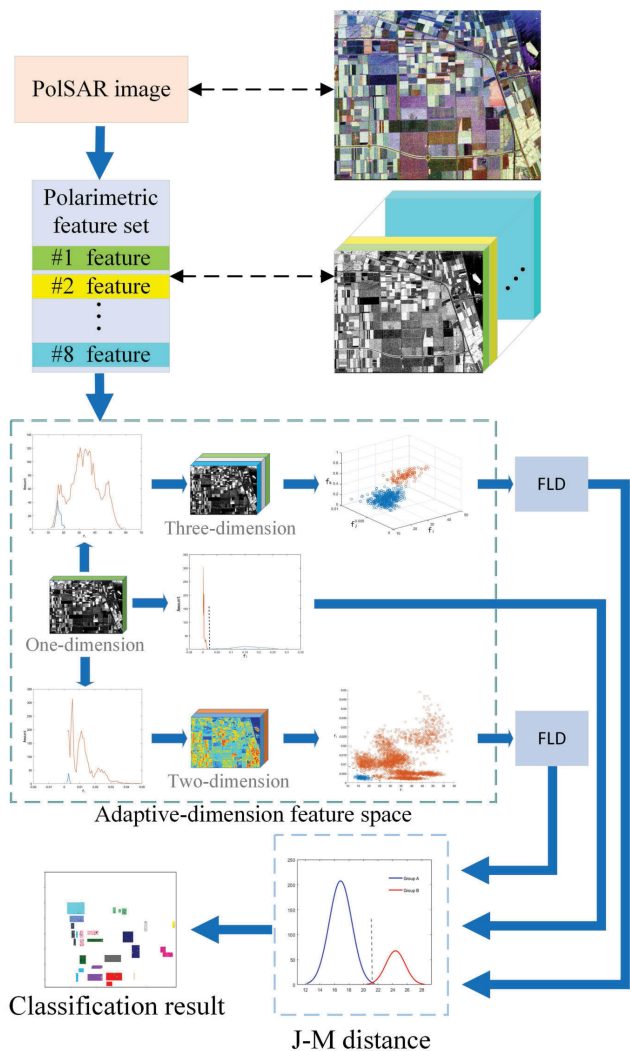
FIGURE 1. Diagram of classification with adaptive-dimension decision tree.

FIGURE 2. Pauli image (left) and ground truth image (right) of Flevoland data.

TABLE 2. Number of labeled pixels and training pixels of AIRSAR data.

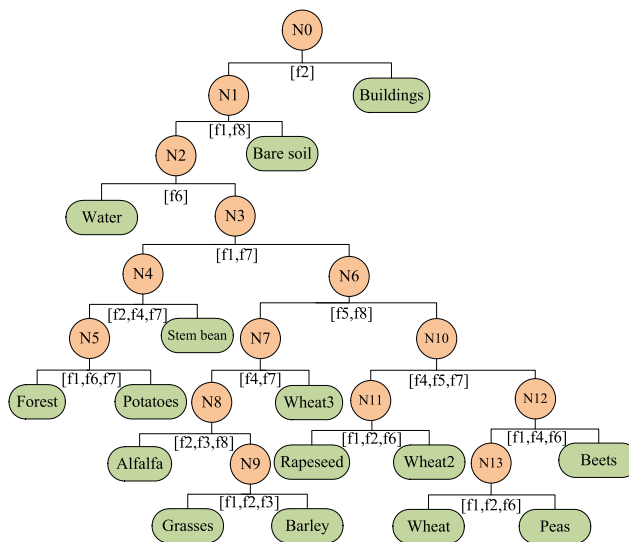|	Stem bean	Forest	Potatoes	Alfalfa	Wheat	Bare soil	Beets	Rapeseed
Labeled pixels	1675	3785	2865	6016	10692	4469	2361	10395
Training pixels	84	189	143	301	535	223	118	520
	Peas	Grasses	Water	Barley	Buildings	Wheat2	Wheat3	
Labeled pixels	4978	2541	779	7315	451	5160	6933	
Training pixels	249	127	39	366	23	258	347	

FIGURE 3. Decision tree of AIRSAR data.

that, those targets with significant differences in the scattering mechanism will be separated firstly with low dimensional polarimetric feature space. As the separation difficulty increases, the number of polarimetric features selected at the decision tree nodes will increase up to two or three, such as N8-N13.

In the structure of the decision tree, the polarimetric features for node classification can be seen visually. Therefore, the polarimetric features are connected with the physical characteristics of the targets, which can explain the role of polarimetric features in classification. For example, the HH backscattering power of the buildings is greater than that of other targets, which could be easily separated by HH scattering power at the node N0. The scattering mechanism of bare soil is similar to surface scattering, but the mean scattering angle is smaller than that of other targets except rapeseed. Considering that the total scattering power of bare soil is also small, hence, with both α and $Span$ bare soil can be discriminated from others. Following that, the water surface is relatively simple with roughness surface scattering, so the entropy value is much smaller than other unclassified targets, thus water can be separated by using the feature $H(1-A)$. Stem bean, forest, and potatoes have dense leaves, so they have volume scattering which could distinguish them from other targets. Usually the volume scattering intensity of stem bean is smaller than that of forest and potatoes. Further research found that $\langle |S_{HH}|^2 \rangle$ can be used to subdivide

article, we replaces a single feature with the adaptive dimensional feature space which adaptively selects the number of dimensions according to the degree of separation difficulty. Here the maximum value of the feature space dimension is increased to three, which enhances the fine-grained interpretation ability of the decision tree.

The branch order of the proposed decision tree for the AIRSAR Flevoland data is shown in Figure 3. It can be seen

stem bean and potatoes, while $\langle |S_{VV}|^2 \rangle$ can be used to subdivide stem bean and forest. Therefore, using P_V, $\langle |S_{HH}|^2 \rangle$, and $\langle |S_{VV}|^2 \rangle$ simultaneously can be more accurate for the separation of stem bean. The scattering angle and canopy scattering intensity of forest are both greater than those of potatoes, also because of the complex scattering phenomenon in the forest area, the entropy value is greater than that of potatoes. Therefore, the simultaneous use of α, $H(1-A)$, and P_V can separate the forest and potatoes. The total scattering power of wheat3, grasses, alfalfa, and barley is much larger than other unclassified targets, hence using *Span* can put them into a group. And since the circular polarization ratio of this group is slightly larger than the unclassified targets, using *CPR* can further improve classification accuracy. The scattering mechanism of beets, peas, and wheat is the combination of surface scattering and volume scattering. However, the co-polarization cross product of beet is smaller than that of wheat and peas. Although the scattering mechanism of peas and wheat is similar, but their HH backscattering ability is significantly different.
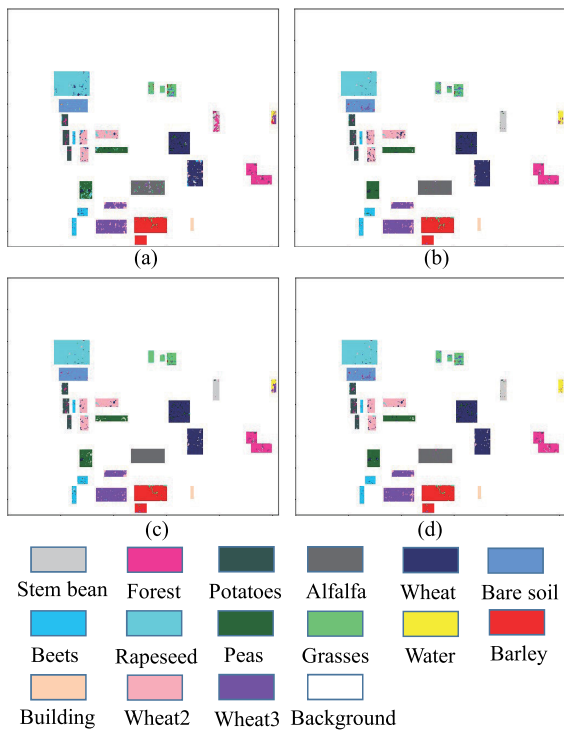

FIGURE 4. Classification result images of one-dimensional feature decision tree(a), two-dimensional feature decision tree(b), three-dimensional feature decision tree(c), and adaptive-dimension feature decision tree(d) of AIRSAR data.

C. CLASSIFICATION ACCURACY

In order to highlight the advantages of the proposed method, based on the same training samples and test samples, classical decision tree, that is the one dimensional polarimetric feature decision tree, as well as two and three-dimensional decision tree and classic Support Vector Machines(SVM) classifier are performed. The images of classification results are shown in Fig. 4. The classification accuracy of five methods

is compared, as shown in Table 3. Because the number of samples is quite different, it is unreasonable to use the total classification accuracy to measure the classification results, so the average accuracy (AA) is used to compare the classification results in this study.

TABLE 3. Comparison of the classification accuracies (%) for AIRSAR data.

	One-dimension	Two-dimension	Three-dimension	SVM	Proposed method
Stem bean	45.13	96.66	97.25	87.64	90.45
Forest	91.70	91.60	90.75	88.85	89.11
Potatoes	88.94	90.30	88.03	86.42	88.10
Alfalfa	93.55	99.10	99.95	91.79	99.22
Wheat	88.48	92.96	93.40	84.23	92.33
Bare soil	99.33	95.12	98.70	97.72	95.12
Beets	91.74	90.39	90.00	85.81	95.30
Rapeseed	93.95	97.05	96.89	96.87	96.89
Peas	82.38	95.20	90.32	78.40	94.42
Grasses	79.65	75.29	88.55	12.90	76.98
Water	42.75	79.46	51.86	95.12	92.94
Barley	96.12	95.61	95.69	85.36	96.30
Buildings	100.00	99.33	99.56	88.03	100.00
Wheat2	88.00	87.85	92.81	82.17	93.06
Wheat3	87.71	91.97	94.16	83.72	91.97
Average Accuracy	**84.63**	**91.86**	**91.20**	**83.00**	**92.81**

As shown in Table 3, the one-dimensional polarimetric feature decision tree has good classification accuracy only for easily separable terrain types, such as bare soil, buildings and so on. However, the classification accuracy of stem beans and water is only 45.13% and 42.75%, respectively. This situation has been greatly improved in the two-dimensional polarimetric feature decision tree, but using two-dimensional feature space caused feature redundancy and reduced classification accuracy for easily separated terrain types, such as buildings and bare soil. It is worth noting that in the classification results of the three-dimensional polarimetric feature decision tree, the classification accuracy of water is only 51.86%, which further indicates that only simply increasing the number of features at the tree nodes will cause the polarimetric feature redundancy and reduce the classification accuracy.

The average classification accuracy of the proposed method is 8.18% higher than that of one-dimensional polarimetric feature decision tree and 0.95% higher than that of two-dimensional polarimetric feature decision tree and 1.61% higher than that of three-dimensional decision tree. It can be seen that the one-dimensional tree has the lowest result, where specific type has very low accuracy; the two-dimensional tree improves the phenomenon a lot; while the three-dimensional tree causes the accuracy lower than the two-dimensional one. Our proposed adaptive dimensional tree achieve the better results than all, especially for those complicated types, but with better interpretability on scattering properties as well as relatively reasonable computation complexity. Although the SVM classifier cannot explain the role of polarimetric features in classification, we still compare

its performance with the proposed method. The average classification accuracy of the proposed method is 9.81% higher than that of SVM. The penalty parameter in SVM is set to 1000 in our experiment.

The experimental environment is as follows: MAC OS operating system, Intel Core i5 processor, 8G memory, Inter Iris Graphics 6100 graphics card and Matlab software. By calculating the running time of the code, it is concluded that the running time of nodes using one-dimensional feature space is about 3.5 seconds, the classification time of nodes using two-dimensional feature space is about 40 times of one-dimensional feature space, about 130 seconds, and the classification time of nodes using three-dimensional feature space is about 2 times of two-dimensional feature space, about 260 seconds. Since the adaptive-dimension polarimetric feature decision tree has seven nodes using three-dimensional feature space, four nodes using two-dimensional feature space and two node using one-dimensional feature space, so the running time is reduced by 28% compared to the three-dimensional decision tree.

Another dataset is empoyled to test the effectiveness of the proposed method. The data is the fully polarimetric C-band image collected by the GaoFen-3 SAR system over the Hulunbuir test site. In this GaoFen-3 data set, four categories are known, including forest, bare land, cole and wheat. According to the unsupervised classification and experience, the other four categories were found, which were assumed to be grasses, water, sand and wetland. The Pauli image and ground truth are shown in Fig. 5. 3% of the labeled pixels were selected as training pixels. The number of samples is shown in Table 4.
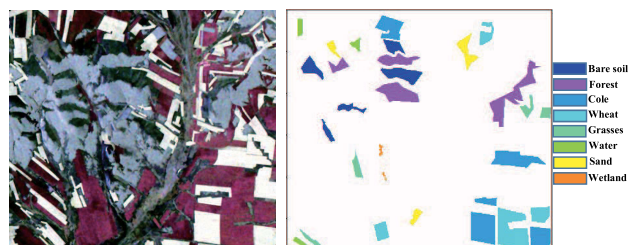

FIGURE 5. Pauli image (left) and ground truth image (right) of GaoFen-3 data.

TABLE 4. Number of labeled pixels and training pixels of GaoFen-3 data.

	Bare soil	Forest	Cole	Wheat	Grasses	Water	Sand	Wetland
Labeled pixels	23038	39099	49588	35121	10214	5382	10213	893
Training pixels	691	1173	1488	1054	306	161	306	27

The experimental environment is the same as the previous data. Fig. 6 gives out the classification results of four methods, and Table 5 indicates the classification accuracies of them. As shown in Table 5, the average classification accuracy of adaptive dimension decision tree is
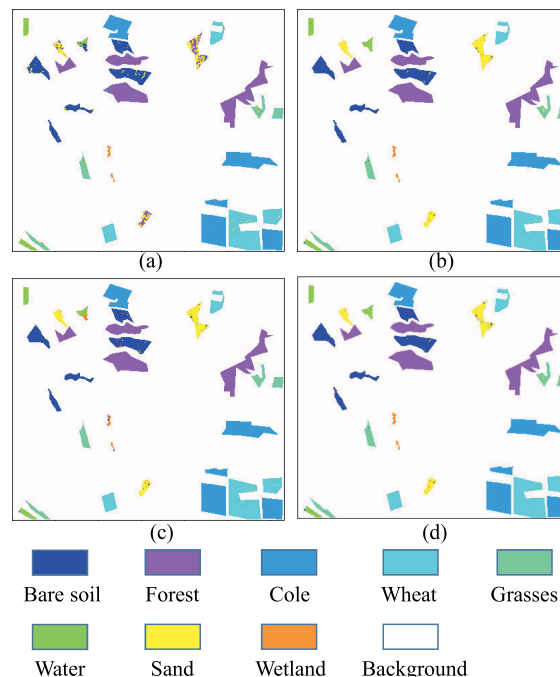

FIGURE 6. Classification result images of one-dimensional feature decision tree(a), two-dimensional feature decision tree(b), three-dimensional feature decision tree(c), and adaptive-dimension feature decision tree(d) of GaoFen-3 data.

TABLE 5. Comparison of the classification accuracies (%) for GaoFen-3 data.

	Bare soil	Forest	Cole	Wheat	Grasses	Water	Sand	Wetland	Average Accuracy
One-dimension	94.77	99.14	99.29	97.9	88.58	86.32	56.02	95.18	**89.65**
Two-dimension	98.74	99.91	99.99	98.92	91.58	92.77	96.19	96.3	**96.80**
Three-dimension	97.76	99.92	99.88	98.77	95.97	80.86	95.09	76.93	**93.15**
SVM	98.72	99.66	99.77	99.15	94.22	94.63	95.29	97.76	**97.40**
Proposed method	98.74	99.91	99.99	99.05	92.82	92.77	96.19	96.3	**96.97**

7.32% higher than that of one-dimensional decision tree and 0.17% higher than that of two-dimensional decision tree. When using the three-dimensional decision tree classification method, the classification accuracy is reduced by 3.82% compared with the proposed method, which is due to redundancy of nodes, which further proves the necessity of adaptive dimension. In this data experiment, SVM achieved a bit higher classification accuracy of 0.43%, since the 8 terrain types here has larger differences between each other, which makes the discrimination much easier. Even from the Pauli image in Fig. 5 the scattering diversity could be observed. However, in the first data experiment, many types all belong to vegetated/agricultural areas with similar scattering characteristics. So the advantage of the proposed approach is more obvious in the previous experimentation. Considering that two-dimensional decision tree runs 40 times of one-dimensional feature space, three-dimensional decision tree runs 80 times of one-dimensional feature space, and because that the adaptive dimension decision tree has one node using three-dimensional feature space and six nodes

using two-dimensional feature space, so the running time is reduced by 43% compared to the three-dimensional decision tree.

From the comparison of classification experiments for all these methods, it could be seen that the proposed decision tree with adaptive dimensional feature space is optimal to other fixed dimensional decision tree approaches, with the consideration of improved classification accuracy and acceptable computation complexity. SVM could achieve similar or a bit lower classification results with our method, however, it could not provide the relation between polarimetric features and the terrain types. Therefore, SVM is not interpretable method, which cannot be extended to other datasets of the same sensor for unsupervised or low-supervised classification. In the following discussion section, the transplantation of polarimetric features obtained by decision tree is implemented. It could not only achieve high classification accuracy, but also save the time for training process.

IV. DISCUSSIONS

A. NECESSITY OF ADAPTIVE DIMENSION FEATURE SPACE

The necessity of using adaptive-dimension feature space for decision tree nodes is demonstrated by classifying bare soil from other targets from Flevoland data set. As shown in Fig. 7, when the bare soil and other targets are classified by the feature f_1 (α) or f_8 (*Span*) respectively, it is difficult to achieve separation of them. However, as shown in Fig. 8, the two-dimensional scatter plots distributed on f_1 and f_8 could clearly separate the bare soil from other targets.
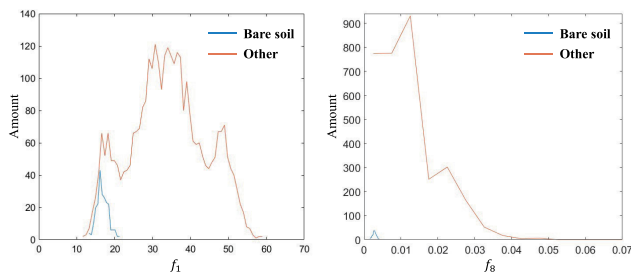
FIGURE 7. Distribution of bare soil and other targets on the feature f_1 (left) or f_8 (right).

On the contrary, for certain terrain types, one single feature is enough to be discriminated from others. As shown in Fig. 9, the complete separation of buildings and other targets can be achieved by the use of only f_2. As shown in Table 3, the classification accuracy of buildings using one-dimensional feature space has reached 100%, but the classification accuracy of buildings using two-dimensional feature space is 99.33%. For this type, by increasing the number of polarization features at the node not only causes an increase in computational complexity, but also reduces the classification accuracy.

Therefore, it is very important to select the feature space dimension at the nodes of decision tree, by means of determining the high and low thresholds of the purity. In order to ensure that the nodes with one-dimensional feature have enough capability for separation, the high threshold is set
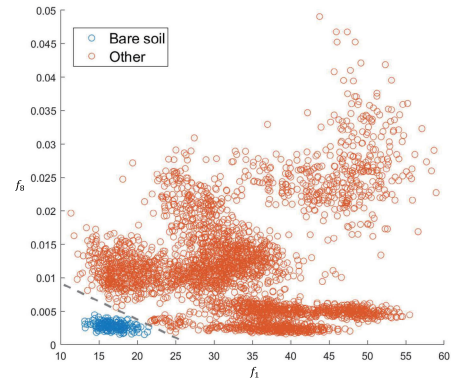
FIGURE 8. Two-dimensional scatter plots distributed on feature f_1 and f_8 of bare soil and other targets.
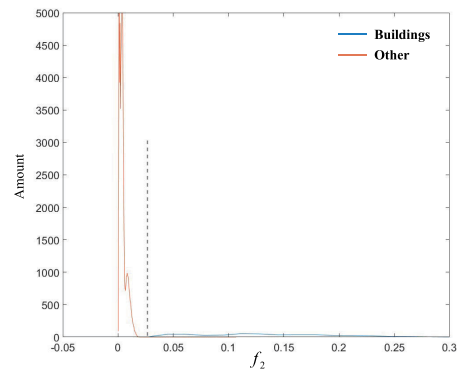
FIGURE 9. Distribution of buildings and other targets on feature f_2.

to "1". When the purity of classification results of training samples is maximum ($= 1$), it loses significance to continue to increase the dimension. The low threshold is set to "0.97" based on experience. When the purity of classification results of training samples is greater than 0.97, the purity can generally reach to 0.99 or even higher after using the two-dimensional feature space. If the purity of classification results of training samples is less than 0.97, it can be considered that the scattering mechanism of the categories is quite similar, which needs to be classified by three-dimensional features. When the selected threshold is too low, the two-dimensional feature space cannot satisfy the classification of some categories. On the contrary, when the selected threshold is too high, the three-dimensional feature space will be used for those easily separated categories, which will increase computational complexity and sometimes decrease accuracy.

B. MIGRATION OF POLARIMETRIC FEATURES

The decision tree classification method based on polarimetric feature is different from the data-driven classification methods. The scattering mechanisms of the targets are described in the classification results. Because the observation capability of the certain POLSAR sensor keeps stable, the polarimetric features for classification can probably be applied to different data using the same sensor without training process. The migration of the proposed method is examined by using
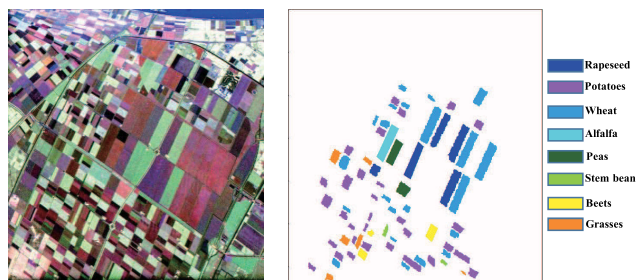
FIGURE 10. Pauli image (left) and ground truth image (right) of Flevoland II data.

TABLE 6. Classification accuracies (%) of Flevoland II.

Node	Categories	Classification accuracy (%)
Node 4	Potatoes	99.90
	Stem bean	98.25
Node 8	Alfalfa	86.73
	Grasses	71.38
Node 10	Rapeseed	99.95
	Beets	100
Node 10	Rapeseed	99.91
	Peas	100
Node 10	Wheat	98.51
	Beets	98.46
Node 10	Wheat	94.16
	Peas	72.21
Node 11	Rapeseed	99.86
	Wheat	99.67
Node 12	Beets	88.27
	Peas	88.66

another AIRSAR data in Flevoland area, as shown in Fig. 10. By comparing the same categories of the two AIRSAR data, the classification of eight categories can be transplanted, this is, rapeseed, potatoes, wheat, alfalfa, peas, stem bean, beets and grasses. The features in the constructed tree nodes are applied directly to the classification of the Flevoland II data without any training process, and the results are shown in Table 6. The decision tree nodes trained by the first AIRSAR data can obtain satisfactory classification accuracy in the second AIRSAR data. High classification accuracies are achieved for all 8 types. It worth to be noted that for those targets with large differences in scattering mechanisms, such as rapeseed and peas, rapeseed and beets, achieve almost complete separation. The type Wheat here corresponds to the type Wheat2 in the first Flevoland data.

V. CONCLUSION

In this article, an adaptive dimension decision tree based on polarimetric feature is proposed, in which the feature space of adaptive dimension is used to replace the fixed one or two or three dimension cases. It not only improves

the fine-grained interpretability of decision trees, but also improves the classification accuracy, with reasonable computation complexity. AIRSAR data in Flevoland area and GaoFen-3 data in Hulunbuir area are used to verify the validity of the method. Compared with the one-dimensional feature decision tree, the classification accuracy of proposed method improves 8.18% in AIRSAR data and 7.32% in GaoFen-3 data. In comparison with the two-dimensional decision tree, the developed approach increases 0.95% and 0.17%. As to the three-dimensional decision tree, the average classification accuracy of proposed method in AIRSAR data is 1.61% higher, while in GaoFen-3 data, it is 3.82% higher. Flexible selection of feature space dimensions can avoid feature redundancy, improve classification accuracy, reduce computational complexity effectively and explain the scattering mechanism of targets more scientifically and completely. In addition, compared with data-driven classification method SVM, with better or equivalent classification accuracy, adaptive dimension decision tree demonstrates its superiority in its interpretability and transplantation capability. Another AIRSAR data in Flevoland area is used to realize the migration of polarimetric feature in terrain classification, and promising results are achieved for all the transportable terrain types.

REFERENCES

[1] H. Anys and D.-C. He, "Evaluation of textural and multipolarization radar features for crop classification," *IEEE Trans. Geosci. Remote Sens.*, vol. 33, no. 5, pp. 1170–1181, Sep. 1995.

[2] Y. Zou, L. Shi, S. Zhang, C. Liang, and T. Zeng, "Oil spill detection by a support vector machine based on polarization decomposition characteristics," *Acta Oceanologica Sinica*, vol. 35, no. 9, pp. 86–90, Sep. 2016.

[3] T.-S. Kim, K.-A. Park, X. Li, A. A. Mouche, B. Chapron, and M. Lee, "Observation of wind direction change on the sea surface temperature front using high-resolution full polarimetric SAR data," *IEEE J. Sel. Topics Appl. Earth Observ. Remote Sens.*, vol. 10, no. 6, pp. 2599–2607, Jun. 2017.

[4] Y. Ji, J. T. S. Sumantyo, M. Y. Chua, and M. M. Waqar, "Earthquake/Tsunami damage level mapping of urban areas using full polarimetric SAR data," *IEEE J. Sel. Topics Appl. Earth Observ. Remote Sens.*, vol. 11, no. 7, pp. 2296–2309, Jul. 2018.

[5] H. Sui, K. An, C. Xu, J. Liu, and W. Feng, "Flood detection in PolSAR images based on level set method considering prior geoinformation," *IEEE Geosci. Remote Sens. Lett.*, vol. 15, no. 5, pp. 699–703, May 2018.

[6] F. Zhang, X. Yao, H. Tang, Q. Yin, Y. Hu, and B. Lei, "Multiple mode SAR raw data simulation and parallel acceleration for Gaofen-3 mission," *IEEE J. Sel. Topics Appl. Earth Observ. Remote Sens.*, vol. 11, no. 6, pp. 2115–2126, Jun. 2018.

[7] D. Haldar, R. Dave, and V. A. Dave, "Evaluation of full-polarimetric parameters for vegetation monitoring in rabi (winter) season," *Egyptian J. Remote Sens. Space Sci.*, vol. 21, pp. S67–S73, Jul. 2018.

[8] L. J. Du and J. S. Lee, "Polarimetric SAR image classification based on target decomposition theorem and complex wishart distribution," in *Proc. IGARSS 96. Int. Geosci. Remote Sens. Symp.*, vol. 1, 1996, pp. 439–441.

[9] J.-S. Lee, M. R. Grunes, T. L. Ainsworth, L.-J. Du, D. L. Schuler, and S. R. Cloude, "Unsupervised classification using polarimetric decomposition and the complex wishart classifier," *IEEE Trans. Geosci. Remote Sens.*, vol. 37, no. 5, pp. 2249–2258, Sep. 1999.

[10] C. Liu, W. Liao, H.-C. Li, K. Fu, and W. Philips, "Unsupervised classification of multilook polarimetric SAR data using spatially variant wishart mixture model with double constraints," *IEEE Trans. Geosci. Remote Sens.*, vol. 56, no. 10, pp. 5600–5613, Oct. 2018.

[11] X. Xue, L. Di, L. Guo, and L. Lin, "An efficient classification method of fully polarimetric SAR image based on polarimetric features and spatial features," in *Proc. 4th Int. Conf. Agro-Geoinformatics (Agro-Geoinformatics)*, Jul. 2015, pp. 327–331.

[12] A. Rezaeian, S. Homayouni, and A. Safari, "Segmentation of polarimetric SAR images usig wavelet transformation and texture features," *Int. Arch. Photogramm., Remote Sens. Spatial Inf. Sci.*, vol. 40, no. 1, p. 613, 2015.

[13] L. Du and J. S. Lee, "Fuzzy classification of Earth terrain covers using complex polarimetric SAR data," *Int. J. Remote Sens.*, vol. 17, no. 4, pp. 809–826, Mar. 1996.

[14] D. H. Hoekman, M. A. M. Vissers, and T. N. Tran, "Unsupervised full-polarimetric SAR data segmentation as a tool for classification of agricultural areas," *IEEE J. Sel. Topics Appl. Earth Observ. Remote Sens.*, vol. 4, no. 2, pp. 402–411, Jun. 2011.

[15] S. Daniel, S. Allain-Bailhache, S. Angelliaume, P. Dubois-Fernandez, and E. Pottier, "Agricultural vegetation classification with SVM and polarimetric SAR data," *Proc. SPIE*, vol. 7824, Oct. 2010, Art. no. 78240L.

[16] T. Zou, W. Yang, D. Dai, and H. Sun, "Polarimetric SAR image classification using multifeatures combination and extremely randomized clustering forests," *EURASIP J. Adv. Signal Process.*, vol. 2010, no. 1, p. 4, Dec. 2009.

[17] P. Du, A. Samat, B. Waske, S. Liu, and Z. Li, "Random forest and rotation forest for fully polarized SAR image classification using polarimetric and spatial features," *ISPRS J. Photogramm. Remote Sens.*, vol. 105, pp. 38–53, Jul. 2015.

[18] L. Jiao and F. Liu, "Wishart deep stacking network for fast POLSAR image classification," *IEEE Trans. Image Process.*, vol. 25, no. 7, pp. 3273–3286, Jul. 2016.

[19] X. Liu, L. Jiao, X. Tang, Q. Sun, and D. Zhang, "Polarimetric convolutional network for PolSAR image classification," *IEEE Trans. Geosci. Remote Sens.*, vol. 57, no. 5, pp. 3040–3054, May 2019.

[20] F. Zhang, J. Ni, Q. Yin, W. Li, Z. Li, Y. Liu, and W. Hong, "Nearest-regularized subspace classification for PolSAR imagery using polarimetric feature vector and spatial information," *Remote Sens.*, vol. 9, no. 11, p. 1114, Nov. 2017.

[21] B. H. Trisasongko, D. R. Panuju, D. J. Paull, X. Jia, and A. L. Griffin, "Comparing six pixel-wise classifiers for tropical rural land cover mapping using four forms of fully polarimetric SAR data," *Int. J. Remote Sens.*, vol. 38, no. 11, pp. 3274–3293, Jun. 2017.

[22] Y. Zhang, J. Zhang, X. Zhang, H. Wu, and M. Guo, "Land cover classification from polarimetric SAR data based on image segmentation and decision trees," *Can. J. Remote Sens.*, vol. 41, no. 1, pp. 40–50, Jan. 2015.

[23] J. Zhang and D. Yan, "A supervised classification method of polarimetric sythetic aperture radar data using watershed segmentation and decision tree c5. 0," *Geomatics Inf. Sci. Wuhan Univ.*, vol. 39, no. 8, pp. 891–896, 2014.

[24] A. Jain and D. Singh, "Decision tree approach to classify the fully polarimetric RADARSAT-2 data," in *Proc. Nat. Conf. Recent Adv. Electron. Comput. Eng. (RAECE)*. Roorkee, India: IIT Roorkee, Feb. 2015, pp. 318–323.

[25] V. Thakur, P. G. N. Ghildiyal, and R. Prakash, "An adaptive technique based on separability index to classify PALSAR data," in *Proc. 2nd Int. Conf. Adv. Comput., Commun., Autom. (ICACCA) (Fall)*, Sep. 2016, pp. 1–8.

[26] G. S. Phartiyal, K. Kumar, D. Singh, and K. P. Singh, "Optimal use of polarimetric signature on PALSAR-2 data for land cover classification," in *Proc. IEEE Int. Geosci. Remote Sens. Symp. (IGARSS)*, Jul. 2017, pp. 4558–4561.

[27] L. Shao and W. Hong, "Decision tree classification of PolSAR image based on two-dimensional polarimetric features," *J. Radars*, vol. 5, no. 6, pp. 681–691, 2016.

[28] L. Deng, Y.-N. Yan, and C. Wang, "Improved POLSAR image classification by the use of multi-feature combination," *Remote Sens.*, vol. 7, no. 4, pp. 4157–4177, Apr. 2015.

[29] W. Hong, L. Shao, and Q. Yin, "Decision hierarchical classification by FLD for vegetation application using PolSAR features," in *Proc. IEEE Int. Geosci. Remote Sens. Symp. (IGARSS)*, Jul. 2017, pp. 5295–5298.

[30] B. Chen, S. Wang, L. Jiao, and S. Zhang, "Unsupervised polarimetric SAR image classification using Fisher linear discriminant," in *Proc. 2nd Asian–Pacific Conf. Synth. Aperture Radar*, Oct. 2009, pp. 738–741.

[31] M. Mahdianpari, B. Salehi, F. Mohammadimanesh, B. Brisco, S. Mahdavi, M. Amani, and J. E. Granger, "Fisher linear discriminant analysis of coherency matrix for wetland classification using PolSAR imagery," *Remote Sens. Environ.*, vol. 206, pp. 300–317, Mar. 2018.

[32] M. Dabboor, S. Howell, M. Shokr, and J. Yackel, "The Jeffries–Matusita distance for the case of complex Wishart distribution as a separability criterion for fully polarimetric SAR data," *Int. J. Remote Sens.*, vol. 35, no. 19, pp. 6859–6873, 2014.

[33] Z. Dong, Q. Zhou, D. Wang, and Z. Chen, "Kharif dryland crop identification based on synthetic aperture radar in the north China plain," in *Proc. 4th Int. Conf. Agro-Geoinformatics (Agro-Geoinformatics)*, Jul. 2015, pp. 38–43.

[34] L. Yi and G. Zhang, "Object-oriented remote sensing imagery classification accuracy assessment based on confusion matrix," in *Proc. 20th Int. Conf. Geoinformatics*, Jun. 2012, pp. 1–8.

[35] Q. Yin, W. Hong, F. Zhang, and E. Pottier, "Optimal combination of polarimetric features for vegetation classification in PolSAR image," *IEEE J. Sel. Topics Appl. Earth Observ. Remote Sens.*, vol. 12, no. 10, pp. 3919–3931, Oct. 2019.

[36] S. Chen, S. Guo, Y. Li, Q. Yin, and W. Hong, "Unsupervised classification based on the logarithmic circular polarization ratio parameter for hybrid polarimetric SAR," in *Proc. IEEE Int. Geosci. Remote Sens. Symp. (IGARSS)*, Jul. 2016, pp. 979–982.

[37] D. H. Hoekman and M. A. M. Vissers, "A new polarimetric classification approach evaluated for agricultural crops," *IEEE Trans. Geosci. Remote Sens.*, vol. 41, no. 12, pp. 2881–2889, Dec. 2003.

[38] A. Kumar and R. K. Panigrahi, "Classification of hybrid-pol data using novel cross-polarisation estimation approach," *Electron. Lett.*, vol. 54, no. 3, pp. 161–163, Feb. 2018.

[39] S. R. Cloude and E. Pottier, "An entropy based classification scheme for land applications of polarimetric SAR," *IEEE Trans. Geosci. Remote Sens.*, vol. 35, no. 1, pp. 68–78, Jan. 1997.

QIANG YIN (Member, IEEE) received the B.E. degree in electronic and information engineering from the Beijing University of Chemical Technology, Beijing, China, in 2004, and the M.S. and Ph.D. degrees in signal and information processing from the Institute of Electronics, Chinese Academy of Science, Beijing, in 2008 and 2016, respectively.

From 2008 to 2013, she was a Research Assistant with the Institute of Electronics, Chinese Academy of Sciences, Beijing. From 2014 to 2015, she was a Research Fellow with European Space Agency, Roma, Italy. She is currently an Associate Professor with the College of Information Science and Technology, Beijing University of Chemical Technology. Her research interests include polarimetric/polarimetric interferometric SAR and deep learning.

JIANDA CHENG received the B.E. degree in automation from the Beijing University of Chemical Technology, Beijing, China, in 2018, where he is currently pursuing the Ph.D. degree with the College of Information Science and Technology.

His research interests include polarimetric SAR processing and artificial intelligence.

FAN ZHANG (Senior Member, IEEE) received the B.E. degree in communication engineering from the Civil Aviation University of China, Tianjin, China, in 2002, the M.S. degree in signal and information processing from Beihang University, Beijing, China, in 2005, and the Ph.D. degree in signal and information processing from the Institute of Electronics, Chinese Academy of Science, Beijing, in 2008.

He is currently a Full Professor of electronic and information engineering with the College of Information Science and Technology, Beijing University of Chemical Technology, Beijing. His research interests include synthetic aperture radar signal processing, image processing, and high-performance computing.

Dr. Zhang has been an Associate Editor of IEEE Access and a Reviewer of the IEEE Transactions on Geoscience and Remote Sensing, the IEEE Journal of Selected Topics in Applied Earth Observations and Remote Sensing, the IEEE Geoscience and Remote Sensing Letters, and the *International Journal of Antennas and Propagation*.

YONGSHENG ZHOU (Member, IEEE) received the B.E. degree in telecommunications engineering from the Beijing Information Science and Technology University, Beijing, China, in 2005, and the Ph.D. degree in signal and information processing from the Institute of Electronics, Chinese Academy of Sciences, Beijing, in 2010.

From 2010 to 2019, he was respectively a Research Assistant and an Associate Research Fellow with the Academy of Opto-Electronics, Chinese Academy of Sciences, Beijing. He is currently a Professor with the College of Information Science and Technology, Beijing University of Chemical Technology, Beijing. His research interests include Pol-InSAR/PolSAR data processing, SAR radiometric calibration and sensor performance analysis, target detection, and recognition.

LUYI SHAO received the B.S. degree in electronic information science and technology from the University of Electronic Science and Technology of China, Chengdu, China, in 2010, and the M.S. and Ph.D. degrees in signal and information processing from the Institute of Electronics, Chinese Academy of Science, Beijing, China, in 2013 and 2018, respectively.

She is currently a Postdoctoral Researcher with the Ocean University of China, Qingdao, China. Her research interests include polarimetric SAR and image classification.

WEN HONG (Senior Member, IEEE) received the M.S. degree in electronic engineering from Northwestern Polytechnical University, Xi'an, China, in 1993, and the Ph.D. degree from Beihang University, Beijing, China, in 1997.

From 1997 to 2002, she was a Faculty Member in signal and information processing with the Department of Electrical Engineering, Beihang University. In between, she was a Guest Scientist with the DLR-HF, Wessling, Germany, from 1998 to 1999 for one year. Since 2002, she has been a Scientist with the Science and Technology on Microwave Imaging Laboratory and a Supervisor of the graduate Student Program and the Administrative Vice Director with the Institute of Electronics, Chinese Academy of Sciences, Beijing. Her main research interests include polarimetric/polarimetric interferometric synthetic aperture radar (SAR) data processing and application, 3-D SAR signal processing, circular SAR signal processing, SAR polarimetry application, and sparse microwave imaging with compressed sensing.

● ● ●